

Influence of Superfluidity on Recombination Reactions of $H + T \rightarrow HT$ and $T + T \rightarrow T_2$ in ${}^3\text{He}$ – ${}^4\text{He}$ Quantum Media under Saturated Vapor Pressure at 1.6 K

Yasuyuki Aratono,^{*,†} Kazunari Iguchi,^{†,‡} Kenji Okuno,[‡] and Takayuki Kumada[†]

Advanced Science Research Center, Japan Atomic Energy Research Institute,
Tokai-mura, Naka-gun, Ibaraki 319-1195, Japan, and Faculty of Science, Shizuoka University,
Ohyu, Shizuoka 422-8529, Japan

Received: July 31, 2002; In Final Form: February 28, 2003

An influence of superfluidity on chemical reaction has been studied in the recombination reactions of hydrogen (H) and tritium (T) atoms, $H + T \rightarrow HT$ and $T + T \rightarrow T_2$, in ${}^3\text{He}$ – ${}^4\text{He}$ mixture solutions at 1.6 K. The reactive species, H and T atoms, were produced in the mixture through the nuclear reaction, ${}^3\text{He} + n \rightarrow p(\text{H}) + T$. Experimental yield ratio of HT to T_2 was 110 ± 17 in normal-fluid solution. However, in superfluid solution, the value decreased to 60 with a decrease in atomic fraction of ${}^3\text{He}$. A two-fluid model was applied to estimate the contribution of superfluidity. The calculated yield of HT to T_2 in the superfluid component became almost a constant value of 56 ± 14 over the whole range of superfluid solution studied. On the basis of preferential formation of HT over T_2 and a computer simulation of relative rate constants, formation of hydrogen isotope bubbles and their tunneling recombination were proposed.

1. Introduction

Since helium is a nonreactive rare gas element, its role in the chemical field has been very minor. Contrary to this, its very unique characters in condensed states have attracted many physicists because of its extremely low temperature, the largest quantum parameter, and so on. The most exciting property of liquid helium is, of course, superfluidity and many investigations have been focused on the phenomena associated with superfluidity itself from a physical point of view.

On the other hand, the influence of quantum properties of liquid and solid helium on physicochemical behaviors of guest atoms and molecules has been one of the current topics because impurities embedded into liquid helium take very unique chemical forms such as a bubble atom, which is produced by the repulsive force between helium and an impurity having an open shell like alkali atoms or in an electronically excited state due to the Pauli exclusion principle, and snowball.^{1–7} The straightforward approach to the above problems is to examine the change of spectroscopic features induced by pressure, temperature, phase transition from normal-fluid to superfluid and so on. Tabbert et al.⁸ investigated the influence of fluidity upon optical transitions of $\text{Ca}(4p\ ^1P_1 \rightarrow 4s\ ^1S_0)$, $\text{Mg}(3p\ ^1P_1 \rightarrow 3s\ ^1S_0)$, and $\text{Ag}(5p\ ^2P_{1/2} \rightarrow 5s\ ^2S_{1/2})$ by a bath cryostat experiment at 1.4–2.4 K, but they could not observe a significant line shift against phase transition at 2.17 K. The recent progress of spectroscopy of molecules picked up into a He-droplet has been giving evidence for superfluidity of helium clusters on the basis of the highly resolved vibrational and rotational spectra.³ However, no experiment has been carried out on the change of spectroscopic features over the phase transition except by Grebenev et al. in a ${}^4\text{He}$ – ${}^3\text{He}$ mixture droplet⁹ because the temperature of the helium cluster is about 0.38 K and cannot be changed easily.

Although several techniques such as laser sputtering, ion beam, hot filament, pick-up by He droplet, etc., have been used for the studies mentioned above,^{2,3} no experiment has been reported on the hydrogen isotopes (H, D, and T) and their molecules (H_2 , HD, D_2 , HT, and T_2). This is a result of difficulties in introducing them into liquid helium and in spectroscopic investigation.

To solve these problems about hydrogen isotopes, the authors developed a nuclear transformation method, ${}^3\text{He}(n,p)\text{T}$, to introduce H and T into liquid helium as well as a radiochemical analysis of the reaction products using radio-gas chromatography^{10,11} and applied this method to the study of the recombination reactions of $H + T \rightarrow HT$ and $T + T \rightarrow T_2$ in liquid helium at 1.6 K.

An attempt to observe the chemical reaction in liquid helium was first reported in the reaction of $\text{Ba} + \text{N}_2\text{O} \rightarrow \text{BaO} + \text{N}_2$ inside helium droplets by Lugovoj et al. in 2000.¹² Although they observed enhancement of the reaction rate in the droplet compared to that in the gas phase, it is not clear how the reaction will be affected by the fluidity.

The purpose of the present study is to investigate the recombination reaction of H and T atoms in superfluid and normal-fluid solutions by the experimental method developed by the authors and make the features of the chemical reaction in superfluid solution clear in comparison with that in normal-fluid solution.

2. Experimental Section

Helium-3 gas was purchased from Isotec Inc. and its isotopic enrichment was more than 99.9 atom %. Tritium content in the gas was below the detection limit for the present T counting system. The mixture gas with predetermined ratio of ${}^3\text{He}$ to ${}^4\text{He}$ (purity of more than 99.99%) was prepared using a glass-made vacuum line operated at 10^{-3} Pa. The superfluid or normal-fluid state was chosen by changing the atomic fraction of ${}^3\text{He}$ (f_{He}) (Figure 1). The experimental setup of the irradiation

* Corresponding author. Tel: +81-29-284-3515. Fax: +81-29-282-5927. E-mail: aratono@popsvr.tokai.jaeri.go.jp.

[†] Japan Atomic Energy Research Institute.

[‡] Shizuoka University.

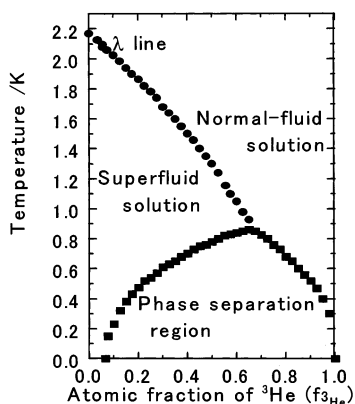


Figure 1. Phase diagram of a ^3He – ^4He mixture solution under saturated vapor pressure.

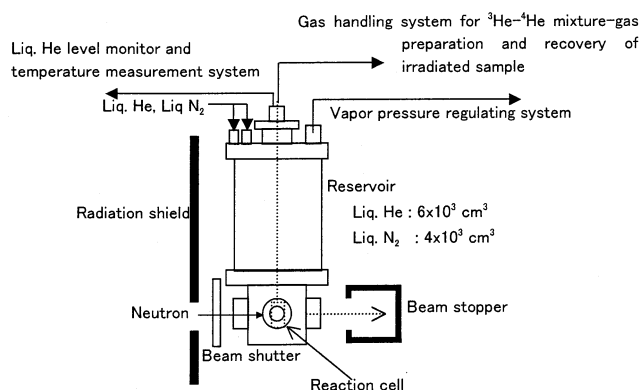


Figure 2. Experimental setup of irradiation apparatus.

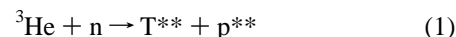
apparatus is shown in Figure 2. The reaction irradiation cell is a stainless steel box with inner dimensions of 2 mm \times 15 mm \times 20 mm. A Polaroid neutron camera with a BC-704 detector (a phosphor screen based on ZnS(Ag) and ^6Li) and Fujifilm FP-3000B was used to monitor the position and condition of the sample under irradiation. Particular attention was paid to keep the reaction cell clean. The mixture gas of ^3He – ^4He with a predetermined ratio was introduced into the reaction cell through a charcoal column cooled at 77 K and lowered to 1.6 K by evaporative cooling of liquid helium. After the vapor pressure attained equilibrium value and the reaction cell was filled with the liquefied mixture, thermal neutron irradiation was performed at the neutron beam guide of JRR-3M (Japan Research Reactor No. 3M)¹³ for about 40 h. The maximum thermal neutron flux measured by the Au-foil activation method was $(3\text{--}4) \times 10^{10} \text{ m}^{-2} \text{ s}^{-1}$. However, in the actual irradiation condition, the average neutron flux changed from $1.43 \times 10^{10} \text{ m}^{-2} \text{ s}^{-1}$ at $f_{^3\text{He}} = 1.0$ to $1.63 \times 10^{10} \text{ m}^{-2} \text{ s}^{-1}$ at $f_{^3\text{He}} = 0.1$. Since the irradiation port is 60 m away from reactor core, the γ -ray dose rate at the irradiation port is very low and radiolysis of the reaction products is negligibly small. After irradiation, the solution was recovered by warming the reaction cell to room temperature and subjecting it to radio-gas chromatographic analysis. The reaction products, HT and T_2 , were separated with a γ -alumina column chilled at 77 K, and their radioactivity was measured by gas flow proportional counter. The atomic fraction of ^3He in the solution was determined with a quadrupole mass spectrometer.

3. Results and Discussion

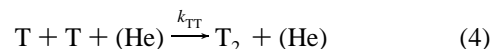
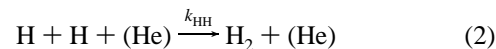
3.1. Thermalization of Energetic Tritium and Proton.

Tritium and protons are produced with recoil energies of 192

and 576 keV, respectively, according to the following nuclear reaction:



where T^{**} and p^{**} show translationally excited states. Tritium is also produced as a bare nucleus, triton(positive charge), because the initial translational velocity of recoil tritium is very much larger than the velocity of a Bohr orbital electron. These species are thermalized efficiently by collisional deactivation with surrounding He owing to close masses among T^{**} , p^{**} , ^3He , and ^4He and to the high density of He. According to the calculation, 100 collisions are sufficient for T^{**} and p^{**} to reach thermal energy at 1.6 K ($1.37 \times 10^{-4} \text{ eV}$). Neutralization of a triton and a proton during the deactivation process in liquid helium has not been well-known. In helium gas, the possibility of neutralized hydrogen isotopes is theoretically predicted due to higher ionization potential of He (24.6 eV) than that for hydrogen isotopes (13.6 eV).¹⁴ However, this prediction is based on the pure charge-transfer process in gas phase. In the present experimental condition, the electrons produced through the deactivation process are considered to play a prominent role for neutralization. Even if a snowball is formed, the mutual reaction of the snowball will be impossible due to the repulsive force because a snowball has positive charge. It will be neutralized to the atomic state at first and then will recombine. After thermalization and neutralization, H and T react with each other to form H_2 , HT, and T_2 by the following recombination reactions:



where k_{HH} , k_{HT} , and k_{TT} are rate constants for each reaction and (He) is a third body for removal of reaction energy released in the recombination reaction.

It has been known that hot H and T atoms, which are produced in the vicinity of the wall, abstract hydrogen from small amounts of hydrogen-containing impurity on the wall of the reaction cell to give H_2 and HT (so-called wall effect). Therefore contribution of H_2 and HT from the wall effect to that from reactions 2 and 3 was estimated as described below.

If the wall effect contributes to the H_2 and HT yield significantly, dependence of the yield on fluidities of the solution will not be observed. From this point of view, the experimental results shown later (Figure 4) qualitatively suggest that the wall effect does not play a significant role in HT formation. To evaluate the wall effect more quantitatively, the fractions of H(proton) and T formed within their recoil ranges from the wall against total H(proton) and total T, H_w and T_w , were evaluated by using neutron intensity and their recoil ranges. The neutron intensity was calculated as a function of depth from the surface to which neutron impinges by the computer code of SRAC.¹⁵ The ranges of proton and T were estimated to be 168 μm for the former and 22 μm for the latter from the stopping power.¹⁶ The values of H_w and T_w were 0.15 and 0.04 at $f_{^3\text{He}} = 1.0$, respectively. In case of $f_{^3\text{He}} = 0.1$, the values of 0.05 and 0.01 were obtained for H_w and T_w , respectively. From the above qualitative and quantitative considerations, it is concluded that the main processes to yield H_2 and HT are reactions 2 and 3.

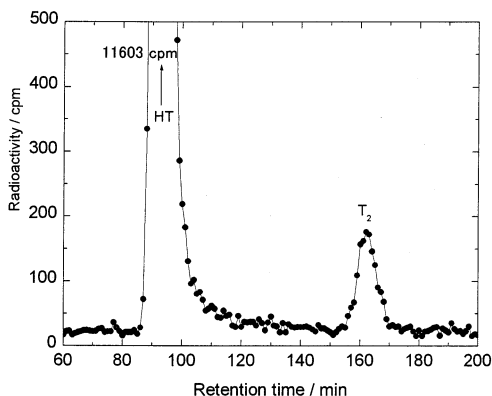


Figure 3. Typical radio-gas chromatogram of neutron-irradiated sample.

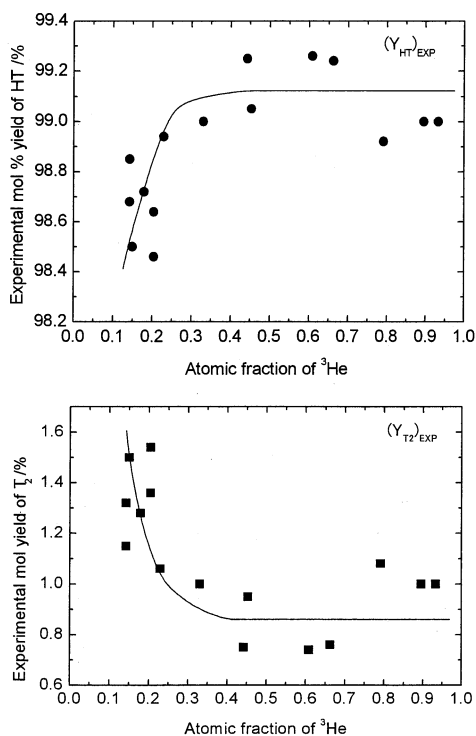


Figure 4. Experimental mol % yield of HT and T_2 against the atomic fraction of ^3He .

3.2. Relative Yields of HT and T_2 Molecules as a Function of the Superfluid Component. Figure 3 shows a typical radio-gas chromatogram of a neutron-irradiated sample. Two peaks were identified as HT and T_2 by the retention time of the standard HT, DT, and T_2 mixture gas. The amount of H_2 could not be analyzed due to very low concentration below the detection limit but is equal to that of T_2 from a material balance.

The experimental mol % yields of HT ($(Y_{HT})_{\text{exp}}$) and T_2 ($(Y_{T_2})_{\text{exp}}$) are presented in Figure 4 as a function of f_{He}^{β} . $(Y_{HT})_{\text{exp}}$ and $(Y_{T_2})_{\text{exp}}$ are defined as follows:

$$(Y_{HT})_{\text{exp}} = \left\{ \frac{\text{(radioactivity of HT)}}{\left[\frac{\text{(radioactivity of HT)} + \text{(radioactivity of } T_2)}{2} \right]} \right\} \times 100$$

$$(Y_{T_2})_{\text{exp}} = \left\{ \frac{\text{(radioactivity of } T_2)}{\left[\frac{\text{(radioactivity of HT)} + \text{(radioactivity of } T_2)}{2} \right]} \right\} \times 100$$

It is interesting to compare Figure 4 with the phase diagram (see Figure 1). As shown in Figure 4, $(Y_{HT})_{\text{exp}}$ and $(Y_{T_2})_{\text{exp}}$ are independent of the atomic fraction of ^3He over $f_{\text{He}}^{\beta} = 0.95$ to

0.35 and begin to change with a decrease in f_{He}^{β} . This turning point corresponds to the transition from normal-fluid solution to superfluid solution at 1.6 K ($f_{\text{He}}^{\beta} = 0.35$, see Figure 1).

It has been reported that OCS and SF_6 in a mixed cluster of $^3\text{He}/^4\text{He}$ are surrounded by a shell of ^4He and that ^3He atoms are on the outside due to the finite size effects.^{9,17} It has been also reported that the phase diagram of the ^3He – ^4He mixture inside the aerogel is different from that of the bulk mixture solution.¹⁸ This was theoretically explained by confinement and substrate– $^3,4\text{He}$ interaction potential effects.¹⁹ Since our results are from a bulk experiment, these effects induced by the environment will not be significant. Thus the present experimental result strongly suggests that superfluidity affects the chemical reaction.

The two-fluid model predicts that liquid ^4He solution below 2.17 K at saturated vapor pressure, He II, is composed of two interpenetrating fluids—normal-fluid and superfluid.²⁰ According to the model, the total density of liquid (ρ) is given by

$$\rho = \rho_n + \rho_s \quad (5)$$

where ρ_n and ρ_s are the densities of normal-fluid and superfluid components and their ratio depends on the temperature. The superfluid does not contribute to the entropy of the liquid and thus thermal phenomena are attributable to the normal-fluid. The model has been successfully applied to the explanation of transport properties of He II. It has been proved by theoretical and experimental studies that a similar picture can be applied to the superfluid solution of the ^3He – ^4He mixture shown in Figure 1. In the case of the mixture solution, the ratio ρ_n/ρ_s depends on both the temperature and the fraction of ^3He . Although the picture of the model is rather based on the physical viewpoints, the entropy, thermal phenomena, and transport properties are closely related to chemical processes. Therefore the authors attempted to apply the model to the experimental results in order to learn how the recombination reaction is influenced by the superfluidity.

As seen in Figure 4, $(Y_{HT})_{\text{exp}}$ and $(Y_{T_2})_{\text{exp}}$ are constant over the whole range of normal-fluid solution ($f_{\text{He}}^{\beta} = 0.95$ – 0.35). This indicates that normal-fluidity does not influence the reaction. On the basis of this experimental fact, the authors assumed that $(Y_{HT})_{\text{exp}}/(Y_{T_2})_{\text{exp}}$ obtained in normal-fluid solution is kept constant over the whole range of ^3He fraction studied and the change of $(Y_{HT})_{\text{exp}}/(Y_{T_2})_{\text{exp}}$ in superfluid solution is attributed to superfluidity. To estimate the contribution of superfluidity, the authors used ρ_n/ρ in ^3He – ^4He mixture solutions at various temperatures under saturated vapor pressures which were obtained experimentally by Pogorelov et al. and Sobolev et al.^{21,22} Figure 5 shows relative densities of normal-fluid and superfluid components, $\rho_n' = \rho_n/\rho$ and $\rho_s' = \rho_s/\rho$, under saturated vapor pressure at 1.6 K.^{21,22} The superfluid component increases with f_{He}^{β} , from 0 at $f_{\text{He}}^{\beta} = 0.35$ to 0.85 at $f_{\text{He}}^{\beta} = 0$.

Experimental yields of HT and T_2 given in Figure 4 can be expressed as follows:

$$(Y_{HT})_{\text{exp}} = (Y_{HT})_n + (Y_{HT})_s = (Y_{HT})\rho_{n'=1} \times \rho_n' + (Y_{HT})_s \quad (6)$$

and

$$(Y_{T_2})_{\text{exp}} = (Y_{T_2})_n + (Y_{T_2})_s = (Y_{T_2})\rho_{n'=1} \times \rho_n' + (Y_{T_2})_s \quad (7)$$

where $(Y_{HT})_n$ and $(Y_{HT})_s$ are yields of HT in normal-fluid and superfluid components at $f_{\text{He}}^{\beta} < 0.35$, and $(Y_{HT})\rho_{n'=1}$ and $(Y_{T_2})\rho_{n'=1}$ are the mean values of $(Y_{HT})_{\text{exp}}$ and $(Y_{T_2})_{\text{exp}}$ at $f_{\text{He}}^{\beta} > 0.35$, respectively. On the basis of eqs 6 and 7, the experimental

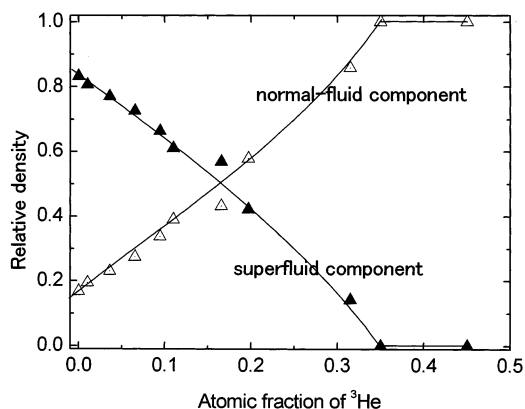


Figure 5. Relative density of superfluid and normal-fluid components in a ^3He – ^4He mixture solution at 1.6 K.

data in Figure 4 were recalculated and the results are plotted in Figure 6. The yield ratios of $(Y_{\text{HT}})_n/(Y_{\text{T}_2})_n = 110 \pm 17$ and $(Y_{\text{HT}})_s/(Y_{\text{T}_2})_s = 56 \pm 14$ were obtained for normal-fluid and superfluid components from Figure 6.

3.3. Proposal of H and T Bubbles and Their Tunneling Recombination. The large yield ratios of HT to T_2 both in superfluid and normal-fluid solutions cannot be explained by a gas-phase reaction where the isotope effect is negligible due to nonbarrier reaction and suggest that reactions 2–4 are the processes having the reaction barrier and proceed through tunneling mechanism because the reactions proceed in the solution at very low temperature. If so, rate constants of the reactions 2–4, k_{HH} , k_{HT} , and k_{TT} , will be very different from each other. The authors attempted to estimate probable rate constants to yield $Y_{\text{HT}}/Y_{\text{T}_2} = 60$ –110 by computer simulation. The rate equations for reactions 2–4 are given by

$$d[\text{H}]/dt = A_{\text{H}} - 2k_{\text{HH}}[\text{H}]^2 - k_{\text{HT}}[\text{H}][\text{T}] \quad (8)$$

and

$$d[\text{T}]/dt = A_{\text{T}} - k_{\text{HT}}[\text{H}][\text{T}] - 2k_{\text{TT}}[\text{T}]^2 \quad (9)$$

where A_{H} and A_{T} are the generation rates of H and T atoms by nuclear reaction and are expressed as follows:

$$A_{\text{H}} = A_{\text{T}} = N\sigma_{\text{th}}f \quad (10)$$

where N is the concentration of ^3He atoms at the experimental point, σ_{th} is the cross section for $^3\text{He}(n,p)\text{T}$ ($5.5 \times 10^{-25} \text{ m}^2$), and f is the neutron flux. Since f is a function of depth at each $f_{^3\text{He}}$, the average value was used at the experimental point. The values of A_{H} ($= A_{\text{T}}$) at $f_{^3\text{He}} = 1.0$ and 0.1, for example, are $2.10 \times 10^{-10} \text{ mol m}^{-3} \text{ s}^{-1}$ and $2.39 \times 10^{-11} \text{ mol m}^{-3} \text{ s}^{-1}$, respectively.

In the above mathematical treatment, the absolute values for k_{HH} , k_{HT} , and k_{TT} cannot be obtained but their ratio, which satisfies $Y_{\text{HT}}/Y_{\text{T}_2} = 60$ –110 and $Y_{\text{H}_2}/Y_{\text{T}_2} = 1$ can be calculated. Since the rate constant of the H–H recombination reaction in liquid helium is expected to be smaller than that in the gas phase, the values less than $2.30 \times 10^7 \text{ m}^3 \text{ mol}^{-1} \text{ s}^{-1}$, which is the mean volume rate constant in the gas phase at around 1 K,^{23,24} were used for calculation. The results were $k_{\text{HH}} > k_{\text{HT}} \gg k_{\text{TT}}$ and differed by one or four orders of magnitude.

The most plausible process with a barrier is considered to be the recombination of H and T atoms in the bubble state. Though the bubble structure of hydrogen isotopes has not been reported, the theoretical calculation seems to predict the hydrogen isotope

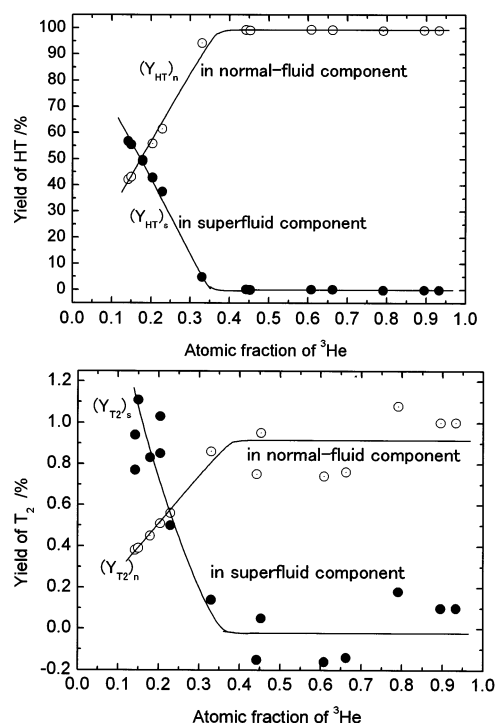


Figure 6. Yield of HT and T_2 in superfluid and normal-fluid components. (Because the superfluid component at $f_{^3\text{He}} > 0.35$ is zero, the scatter of the values around the yield of 0 is due to variation of experimental values.)

bubbles. Saarela and Krotscheck²⁵ calculated the radial distribution functions of D and T atoms and effective masses of hydrogen isotopes in liquid ^4He . According to the radial distribution function, the nearest-neighbor peaks of D and T atoms are moved from about 0.35 nm for He–He to about 0.4 nm for both He–D and He–T. Although the distribution function of H is not given due to the lack of convergence of their iteration scheme for the Euler equation below 10 atm, the equilibrium distance of the He–H pair potential is around 0.36 nm and is longer than that of ^4He – ^4He due to a short-range repulsive force.^{26,27} The effective mass of hydrogen isotopes in liquid helium is roughly 10 for H, D, and T atoms.²⁵ On the basis of these calculations, we can briefly draw a picture of the ground state of a hydrogen isotope bubble in liquid helium as a radius of about 0.4 nm, effective mass of about 10, the spherical square well potential a result of the s structure of the valence electron, and lower ground state for T than H a result of lower zero-point energy.

The formation of a bubble of impurity embedded into liquid helium has been well established for electron and some alkali and alkaline-earth elements by theoretical and experimental investigations.² For example, the electron resides in the square well potential of about 1 eV in depth with the bubble radius of 1.72 nm at zero pressure at 1.3 K.²⁸ The radius of a Cs bubble at 1.5 K under saturation vapor pressure is experimentally obtained to be 0.65 nm and coincides well with the theoretical calculation employing the pair potential of the Lennard-Jones form.^{29,30}

In order for hydrogen isotopes in the bubble state to recombine, the barrier should be overcome either by thermal motion or tunneling. If the dissociation energy in the H–He pair potential is taken as a measure of minimum activation energy as the first approximation, 7–8 K would be necessary for the bubble–atom reaction.^{26,27} Since the reaction temperature is 1.6 K, it seems reasonable to consider that reactions 2–4

proceed through the tunneling process. Since the zero-point energy of T is lower than that of H, the tunneling distance for reaction 4 would be longer than that of reaction 3. This would result in the preferential formation of HT over T₂ in liquid helium, being different from the volume recombination reaction mechanism in the gas phase at around 1 K.

It has been supposed that the neutralization process between Ba⁺ and the electron in liquid helium proceeds via the tunneling mechanism.^{2,31,32} Since the neutralization process has no reaction barrier in general, the bubble state of the reactants is considered to be responsible for the tunneling reaction. In fact, their bubble states in liquid helium are strongly supported by optical investigations.^{8,28,33}

3.4. Reactivity in Superfluid and Normal-fluid Solutions.

The different preference in formation of HT and T₂ over phase transition from normal-fluid to superfluid solutions, $\{(Y_{\text{HT}})_n / (Y_{\text{T}_2})_n\} / \{(Y_{\text{HT}})_s / (Y_{\text{T}_2})_s\} \approx 2$, is the next point of interest. Two factors seem to influence the results. One is the change of bubble structure against the atomic fraction of ³He, and the other one is coherence of the system.

The total energy of the bubble atom, E_t , is given by following equation:^{34,35}

$$E_t = E_{\text{fa}} + E_{\text{int}} + E_c \quad (11)$$

where E_{fa} is the electronic energy of the free atom, E_{int} is the energy of the interaction with the surrounding helium atoms, and E_c is the energy to form the bubble atom. As the first approximation, E_c is expressed by the sum of surface energy (E_{surf}) and pressure volume work (E_{pv}),

$$E_c = E_{\text{surf}} + E_{\text{pv}} = 4\pi R_b^2 \sigma + [4\pi R_b^3 / 3] p \quad (12)$$

where R_b , σ , and p represent radius of bubble, surface tension, and pressure of liquid helium. In the present experimental conditions, these parameters vary with f_{He}^{A} and it may lead to the change of total energy of the bubble. However, $(Y_{\text{HT}})_{\text{exp}}$ and $(Y_{\text{T}_2})_{\text{exp}}$ are constant over the wide range of $f_{\text{He}}^{\text{A}} = 0.95$ to 0.35 and thus drastic change in its structure at $f_{\text{He}}^{\text{A}} = 0.35$ to 0.1 would not be expected. Therefore the bubble structure might not exert a substantial effect upon the yield ratios of HT to T₂ both in superfluid and normal-fluid solutions. This seems to be consistent with a spectroscopic study by Tabbert et al. who did not observe change of spectroscopic features of Ca, Mg, and Ag in the bubble state upon phase transition from superfluid to normal-fluid.⁸

Recently, Kumada et al. studied the H–H recombination reaction in quantum solid *p*-H₂ which contains various amount of *o*-H₂ by ESR, ENDOR, and ESE at 4.2 K.³⁶ They changed relative concentration of *o*-H₂ (x_0) from 0.001 to 0.75 (normal H₂) and found that the reaction is controlled by different mechanisms, depending on the concentration of *o*-H₂. At $x_0 > 0.1$, the reaction was well explained by the usual diffusion-controlled process. However, at concentrations lower than 0.1, the reaction proceeded with a much slow rate than expected from the diffusion coefficient. They attributed the absence of recombination of H atoms in highly purified solid *p*-H₂ to the lack of an energy dissipation path due to high coherence of the matrix. Though the reaction media are different each other, the results at $f_{\text{He}}^{\text{A}} < 0.35$ in the present experiment and those by Kumada et al. at $x_0 < 0.1$ seem to be common from the viewpoint of the phenomena observed in high coherent quantum media.

Lugovoj et al. studied the rate of the chemiluminescent Ba + N₂O → BaO + N₂ reaction inside a superfluid He-droplet-

(0.38 K) spectroscopically and found great enhancement of the reaction rate over the gas-phase reaction.¹² Though they could not compare the reaction rate with that in normal-fluid solution due to experimental difficulty in making normal-fluid He-droplet, the results obtained both in the authors' work and in their experiment predict very unique features of the chemical reactions in superfluid solution.

4. Conclusion

Chemistry in quantum media has been gaining attention as a field of low-temperature chemistry.³⁷ Liquid and solid hydrogen constitute one of the typical quantum media, and chemical reactions in the solid hydrogen have been widely investigated focusing on the tunneling phenomena in chemical reactions.^{38–40} The quantum parameter of helium is 2–3 times larger than that of hydrogen⁴¹ and hence many physicochemical effects associated with quantum character, especially with superfluidity, will be expected. Chemical phenomena concerning hydrogen isotopes are very fundamental and thus the chemical behavior of hydrogen isotopes in liquid helium will lead to a very unique field of low-temperature chemistry. From this point of view, investigations of temperature and pressure effects upon recombination reactions of H and T atoms in superfluid and normal-fluid solutions are in progress by the radiochemical methods developed by the authors.

Acknowledgment. The authors thank Mr. B. Komukai and Dr. S. Kubo for their extensive advice in computer calculations of neutron intensity and rate equations. The authors also express their appreciation to Drs. S. Shimizu and M. Nomura for their helpful discussions.

References and Notes

- (1) Proceedings of the 128th WE-Heraeus-Seminar on Ions and Atoms in Superfluid Helium. *Z. Phys. B* **1995**, *98*, 296.
- (2) Tabbert, B.; Günther, H.; zu Putlitz, G. *J. Low Temp. Phys.* **1997**, *109*, 653.
- (3) Toennies, P. J.; Vilesov, A. F. *Annu. Rev. Phys. Chem.* **1998**, *49*, 1.
- (4) Takahashi, N.; Shigematu, T.; Shimizu, S.; Horie, K.; Hirayama, Y.; Izumi, H.; Shimoda, T. *Physica B* **2000**, *284*, 89.
- (5) Kwon, Y.; Huang, P.; Patel, M. V.; Blume, D.; Whaley, K. B. *J. Chem. Phys.* **2000**, *113*, 6469.
- (6) Fujisaki, A.; Sano, K.; Kinoshita, T.; Takahashi, Y.; Yabusaki, T. *Phys. Rev. Lett.* **1993**, *71*, 1039.
- (7) Takami, M. *Comments At. Mol. Phys.* **1996**, *32*, 219.
- (8) Tabbert, B.; Beau, M.; Günther, H.; Haußler, W.; Hönninger, C.; Meyer, K.; Plegemann, B.; zu Putlitz, G. *Z. Physica B* **1995**, *97*, 425.
- (9) Grevenev, S.; Toennies, J. P.; Vilesov, A. F. *Science* **1998**, *279*, 2083.
- (10) Aratono, Y.; Matumoto, T.; Kumada, T.; Takayanagi, T.; Komaguchi, K.; Miyazaki, T. *J. Phys. Chem. A* **1998**, *102*, 1501.
- (11) Iguchi, K.; Kumada, T.; Okuno, K.; Aratono, Y. *Chem. Phys. Lett.* **2001**, *349*, 421.
- (12) Lugovoj, E.; Toennies, J. P.; Vilesov, A. *J. Chem. Phys.* **2000**, *112*, 8217.
- (13) Kawabata, Y.; Suzuki, M.; Takahashi, H.; Onishi, N.; Shimanuki, A.; Sugawa, Y.; Niino, N.; Kasai, T.; Funasho, K.; Hayakawa, S.; Okuhata, K. *J. Nucl. Sci. Technol.* **1990**, *27*, 1138.
- (14) Wolfgang, R. *The Hot Atom Chemistry of Gas-Phase Systems. In Progress in Reaction Kinetics*; Porter, G., Ed.; Pergamon Press: Elmsford, NY, 1965; Vol. 3, p 97.
- (15) Tsuchihashi, K.; Ishiguro, Y.; Kaneko, K.; Ido, M. *JAERI-1302* **1986**.
- (16) Ziegler, J. F. *Stopping Powers and Ranges in all Elements*; Pergamon Press: Elmsford, NY, 1977; Vols. 3 and 4.
- (17) Barranco, M.; Pi, M.; Gatica, S. M.; Hernández, E. S.; Navarro, J. *Phys. Rev. B* **1997**, *56*, 8997.
- (18) Kim, S. B.; Ma, J.; Chan, M. H. W. *Phys. Rev. Lett.* **1993**, *71*, 2268.
- (19) Pricapenko, L.; Treiner, J. *Phys. Rev. Lett.* **1995**, *74*, 430.
- (20) Dobbs, E. R. *Helium Three*; Oxford University Press Inc.: New York, 2000.

- (21) Pogorelov, L. A.; Esel'son, B. N.; Nosovitsukaya, O. S.; Sobolev, V. I. *Sov. J. Low Temp. Phys.* **1979**, *5*, 40.
- (22) Sobolev, V. I.; Esel'son, B. N.; Nosovitsukaya, O. S.; Pogorelov, L. A. *Sov. J. Low Temp. Phys.* **1979**, *5*, 269.
- (23) Hyden, M. E.; Hardy, W. N. *J. Low Temp. Phys.* **1995**, *99*, 787.
- (24) Arai, T.; Yamane, M.; Fueki, A.; Mizusaki, T. *J. Low Temp. Phys.* **1998**, *373*, 112.
- (25) Saarela, M.; Krotscheck, E. *J. Low Temp. Phys.* **1993**, *90*, 415.
- (26) Silvera, I. F. *Phys. Rev.* **1984**, *29*, 3899.
- (27) Partridge, H.; Bauschlicher, C. W., Jr. *Mol. Phys.* **1999**, *96*, 705.
- (28) Grimes, C. C.; Adams, G. *Phys. Rev. B* **1990**, *41*, 6366.
- (29) Bauer, H.; Beau, M.; Friedl, B.; Marchand, C.; Miltner, K.; Reyher, H. *J. Phys. Lett.* **1990**, *146*, 134.
- (30) Kürten, K. E.; Ristig, M. L. *Phys. Rev.* **1983**, *27*, 5479.
- (31) Bauer, H.; Beau, M.; Bernhardt, A.; Friedl, B.; Reyher, H. *Phys. Lett.* **1989**, 137.
- (32) Beau, M.; zu Putlitz, G.; Tabbert, B. *Z. Phys. B* **1996**, *101*, 253.
- (33) Reyher, H. J.; Bauer, H.; Huber, C.; Mayer, R.; Schafer, A.; Winnacker, A. *Phys. Lett. A* **1986**, *115*, 238.
- (34) Jortner, J.; Kestner, N. R.; Rice, S. A.; Cohen, M. H. *J. Chem. Phys.* **1965**, *43*, 2614.
- (35) Hiroike, K.; Kestner, N. R.; Rice, S. A.; Jortner, J. *J. Chem. Phys.* **1965**, *43*, 2625.
- (36) Kumada, T.; Sakakibara, M.; Nagasaka, T.; Fukuta, H.; Kumagai, J.; Miyazaki, T. *J. Chem. Phys.* **2002**, *116*, 1109.
- (37) *Proceedings of the 3rd International Conference on Low Temperature Chemistry*; Nagoya, Japan, 1999.
- (38) Kumada, T.; Komaguchi, K.; Aratono, Y.; Miyazaki, T. *Chem. Phys. Lett.* **1996**, *261*, 463.
- (39) Shevtsov, V.; Kumada, T.; Aratono, Y.; Miyazaki, T. *Chem. Phys. Lett.* **2000**, *319*, 535.
- (40) Kumada, T.; Kumagai, J.; Miyazaki, T. *J. Low Temp. Phys.* **2001**, *122*, 265.
- (41) Silvera, I. F. *Rev. Mod. Phys.* **1980**, *52*, 393.